

Supporting information

Modeling TADF: the role of the matrix polarizability

D. K. Andrea Phan Huu^a, Sangeeth Saseendran^a, and Anna Painelli^a

^a*Department of Chemistry, Life Sciences and Environmental Sustainability, Parma University, 43124 Parma, Italy.*

1 Estimating spin-orbit coupling matrix elements

Symbols in Fig. S1 show squared modulus of the S_1 - T_1 coupling as a function of the conformational coordinate (see ref. 35 for details). To simulate this quantity we diagonalized the molecular Hamiltonian (Eq. 2 main text) neglecting the spin-orbit coupling (SOC). We also disregard the coupling to molecular vibrations (TD-DFT calculations are done at fixed geometry) and diagonalize the electronic Hamiltonian for fixed δ . In the singlet subspace we obtain S_0 and S_1 as follows:

$$\begin{aligned} |S_0\rangle &= \sqrt{1-\rho}|N\rangle + \sqrt{\rho}|Z\rangle \\ |S_1\rangle &= \sqrt{\rho}|N\rangle - \sqrt{1-\rho}|Z\rangle \end{aligned} \quad (1)$$

where:

$$\rho = \frac{1}{2} \left[1 - \frac{z}{\sqrt{z^2 + \tau^2}} \right] \quad (2)$$

where $\tau = \tau_0 |\sin \delta|$

In the triplet subspace we obtain T_1 and T_2 as:

$$\begin{aligned} |T_1\rangle &= \sqrt{1-\sigma}|T\rangle + \sqrt{\sigma}|L\rangle \\ |T_2\rangle &= \sqrt{\sigma}|T\rangle - \sqrt{1-\sigma}|L\rangle \end{aligned} \quad (3)$$

where

$$\sigma = \frac{1}{2} \left[1 - \frac{k-z}{\sqrt{(k-z)^2 + \beta^2}} \right] \quad (4)$$

where $\beta = \beta_0 |\sin \delta|$.

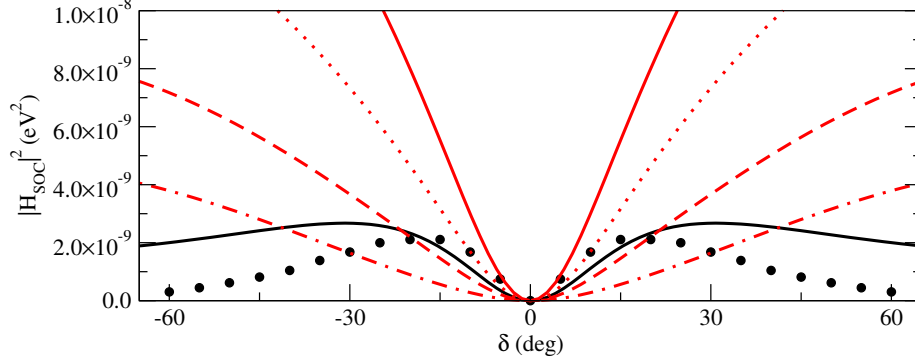


Figure S1: The square modulus of the S_1 - T_1 SOC matrix element vs the conformational coordinate. Black circles show TD-DFT results, from ref. 35. The black line show the best fit obtained in ref. 35 setting $V_{SOC} = 3.84 \times 10^{-4}$ eV and $W_{SOC} = 1.74 \times 10^{-4}$ eV. Red lines show results for the same V_{SOC} value, but for negative W_{SOC} . Specifically: $W_{SOC} = -1.5 \times 10^{-4}$ eV (continuous line), $W_{SOC} = -1.0 \times 10^{-4}$ eV (dotted line), $W_{SOC} = -0.5 \times 10^{-4}$ eV (dashed line), $W_{SOC} = -0.1 \times 10^{-4}$ eV (dot-dashed line).

We are now in the position to calculate the SOC matrix elements

$$\begin{aligned} \langle S_0 | \hat{H}_{SOC} | T_1 \rangle &= \sqrt{1-\rho}\sqrt{1-\sigma}V_{SOC} + \sqrt{\rho}\sqrt{\sigma}W_{SOC} \\ \langle S_1 | \hat{H}_{SOC} | T_1 \rangle &= \sqrt{\rho}\sqrt{1-\sigma}V_{SOC} - \sqrt{1-\rho}\sqrt{\sigma}W_{SOC} \end{aligned} \quad (5)$$

At $\delta = 0$, $\beta = \tau = 0$ and $\rho = \sigma = 0$ so that the value of $\langle S_0 | \hat{H}_{SOC} | T_1 \rangle$ at $\delta = 0$ fixes the (absolute value of) $V_{soc} = 3.84 \times 10^{-4}$ eV. In ref. 35 we estimated $W_{SOC} = 1.74 \times 10^{-4}$ eV as to best reproduce the δ -dependence of $|\langle S_1 | \hat{H}_{SOC} | T_1 \rangle|^2$ (see the black line in Fig. S1. However in that work we implicitly imposed that the V_{SOC} and W_{SOC} had the same sign (their absolute sign is irrelevant, but having the two with the same or opposite sign leads to different results. The red curves in Fig. S1 are obtained imposing opposite sign for the two SOC matrix elements: it is clear that results are untenable leading to a monotonous increase of $|\langle S_1 | \hat{H}_{SOC} | T_1 \rangle|^2$ with $|\delta|$.

2 Non-adiabatic approach to conformational degrees of freedom

The dimensionless conformational coordinate $\hat{\delta}$ can be expressed in second quantization as

$$\hat{\delta} = (\hat{a}^\dagger + \hat{a}) \quad (6)$$

where \hat{a}^\dagger (\hat{a}) is the creation (annihilation) operator of a vibrational quantum. In the implementation of the calculation, in order to write the Hamiltonian in

terms of the creation and annihilation operators, we expand $|\sin(\delta)|$ up to the third order, as to be consistent with the quartic expansion of the potential. Specifically:

$$\sin \delta \sim \delta + \frac{1}{6}\delta^3 \quad (7)$$

We observe that the sign of the mixing matrix elements, τ and β is irrelevant, so we can neglect the absolute value in Eq. 1 (main text).

3 Contributions to the RISC and ISC rates

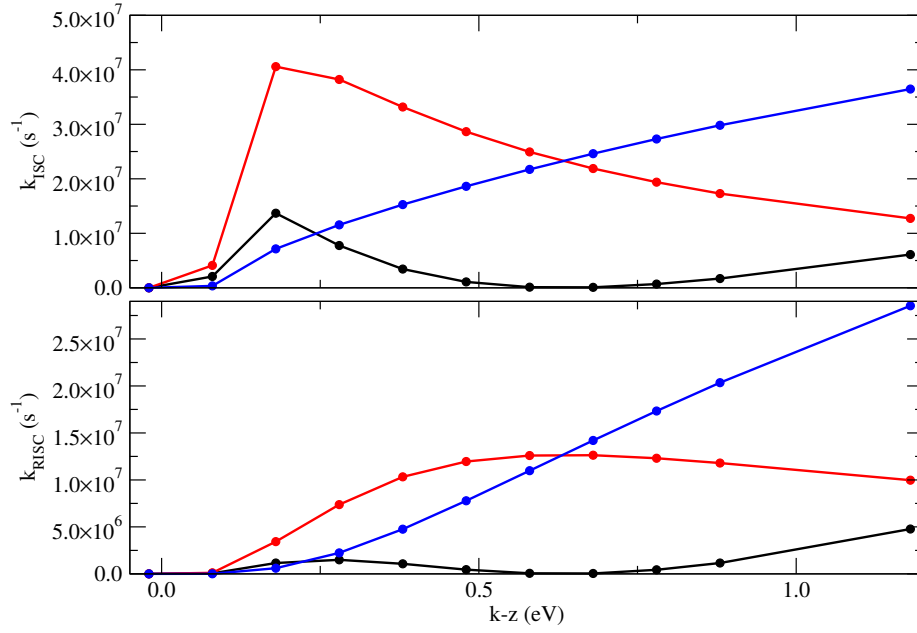


Figure S2: The dependence of the RISC and ISC rates calculated for the standard model (black symbols) and setting either V_{SOC} or W_{SOC} to zero (blue and red symbols, respectively).

4 RISC rates: the Marcus model

The Marcus approach, as applied to RISC rates, relies on the adiabatic solution of the molecular Hamiltonian in Eq. 2. Neglecting the kinetic energy associated to the conformational and vibrational coordinate, the diagonalization of the adiabatic Hamiltonian leads to δ and Q -dependent energies for the four electronic states. Fig S3 shows the resulting potential energy surfaces for the S_1 and T_1 states. The two surfaces are degenerate at $\delta = 0^\circ$ where the SOC vanishes, $|\langle S_1 | H_{SOC} | T_1 \rangle| = 0$. The equilibrium position for the triplet state is found at $\delta = 22^\circ$ and $Q = 1.68$ with energy $E_T = 3.2217$ eV. The singlet minimum is found at $\delta = 0^\circ$ and $Q = 1.92$ with energy $E_S = 3.2700$ eV. The singlet-triplet minimum $\Delta E_{ST} = 0.0485$ eV coincides with the relaxation energy and the activation energy, so that

$$k_{RISC} = \frac{2\pi}{\hbar} \frac{|\langle S_1 | H_{SOC} | T_1 \rangle|^2}{\sqrt{4\pi\Delta_{ST}k_B T}} \exp\left\{-\frac{\Delta E_{ST}}{k_B T}\right\} \quad (8)$$

where k_B is the Boltzmann constant. The delicate point is the SOC matrix elements. Indeed the Marcus model is defined on diabatic states, with constant interaction. Here instead we are trying to apply the model to the adiabatic states and $|\langle S_1 | H_{SOC} | T_1 \rangle|$ varies with the molecular geometry. Specifically, at the crossing point $|\langle S_1 | H_{SOC} | T_1 \rangle| = 0$, while at the equilibrium geometry for the triplet state $|\langle S_1 | H_{SOC} | T_1 \rangle| = 2.66 \times 10^{-5}$ eV. Of course the RISC rate vanishes exactly if the SOC is fixed at the value relevant to the crossing point. Fig. S4 shows RISC rates calculated with the above equation setting the SOC matrix element to the value calculated at the triplet geometry. Corresponding ISC rates are then estimated imposing the detailed balance.

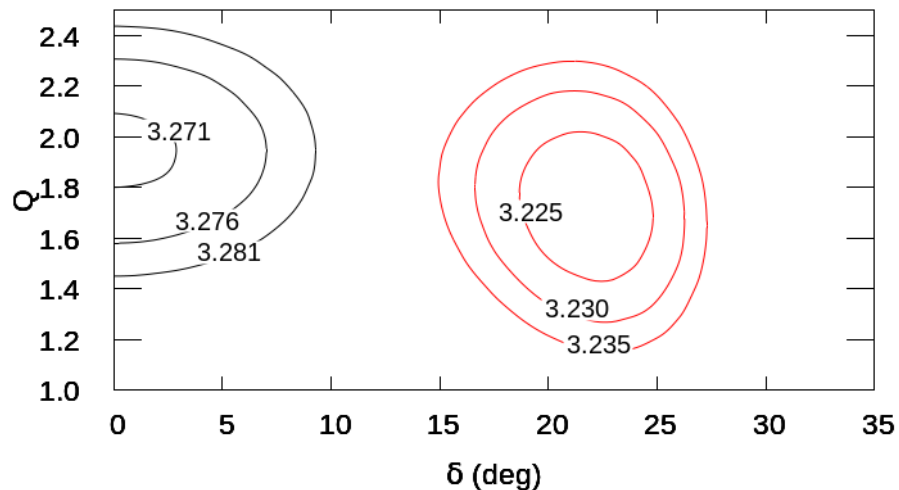


Figure S3: Contour plots of the adiabatic potential energy surfaces (eV) relevant to T_1 (red) and S_1 (black) states.

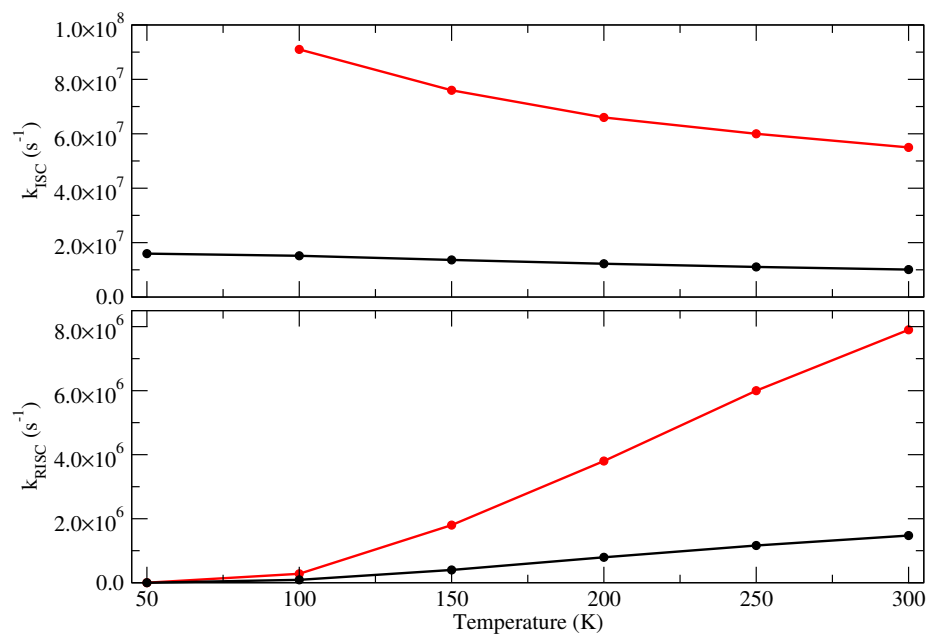


Figure S4: The temperature dependence of the RISC and ISC rates calculated for the standard model (black symbols) and in the Marcus model fixing the SOC matrix elements to the value relevant to the equilibrium geometry for the triplet state (red symbols). Setting the SOC matrix element to the value relevant to the singlet-triplet crossing point both RISC and ISC rate would vanish.

5 Comparison with PCM non-equilibrium formalisms

Table S1: Excitation energy for S_1 and T_1 computed in the effective model (EM) and at the TDA-M06-2X/6-31G(d) level. All results refer to vertical transition energies at the ground state equilibrium geometry. Two dielectric media are considered with $\epsilon_{opt} = \epsilon_{st}=2.6$ and 3, as specified in parentheses. In EM environmental effects are accounted for via an antiadiabatic solvation model (refs. 32, 34). TD-DFT results are obtained in the non-equilibrium PCM solvation formalisms, in the three flavors available in Gaussian16 [ref. 47]: linear response (LR), corrected linear response (cLR) and external iteration (EI). All values are in electronvolts.

	S_1	T_1
gas phase EM	3.44	3.44
gas phase TDA-DFT	3.4523	3.4461
EM (2.6)	3.14	3.14
PCM-LR (2.6)	3.5038	3.4973
PCM-cLR (2.6)	3.1262	3.1231
PCM-EI (2.6)	2.4196	2.4180
EM (3.0)	3.10	3.10
PCM-LR (3.0)	3.5087	3.5021
PCM-cLR (3.0)	3.0884	3.0857
PCM-EI (3.0)	2.3020	2.3007